Current Plant Biology 38 (2024) 100354

Contents lists available at ScienceDirect

Current Plant Biology

journal homepage: www.elsevier.com/locate/cpb

CRISPR/Cas9 edited *StbHLH47* lines exhibit altered expression profiling of iron regulating genes and increased iron content in *Solanum tuberosum*☆

Hanny Chauhan [a], Anshu Alok [b], Aiana [a], Santosh K. Upadhyay [c], Ashutosh Pandey [d], Kashmir Singh [a,*]

[a] Department of Biotechnology, BMS Block I, Panjab University, Sector 25, Chandigarh 160014, India
[b] Department of Plant Pathology, University of Minnesota, Saint Paul, MN 55108, USA
[c] Department of Botany, Panjab University, Sector 14, Chandigarh 160014, India
[d] National Institute of Plant Genome Research, Aruna Asaf Ali Marg, New Delhi 110067, India

ARTICLE INFO

Keywords:
CRISPR/Cas9
BHLH47 transcription factor
Iron homeostasis
POPEYE
ICP-MS

ABSTRACT

Iron is an essential plant nutrient, and a continuous supply of it is required as it is a key factor in various metabolic processes, including photosynthesis, chlorophyll synthesis, and respiration. Various transcription factors are known to regulate iron homeostasis in plants, and the *bHLH* transcription factor family is one of them. The *StbHLH47* is a homologue of the *Arabidopsis POPEYE* (*PYE*), which is known to repress iron homeostasis-related genes in *Arabidopsis*. Potato is the most consumed vegetable in the world and is low in iron content. We have generated CRISPR/Cas9-edited *StbHLH47* lines and performed a detailed analysis of these lines. The analysis revealed that the roots of *StbHLH47* edited lines have decreased ferric chelate reductase (FCR) activity compared to the roots of the wild-type (WT) plant. We also observed that CRISPR/Cas9 edited lines have fewer trichomes when compared to the WT plant. The expression of genes associated with iron homeostasis was also measured. Compared to the control, the expression of *StbHLH47* was downregulated in the edited lines, while the expression of *StNAS4*, *StOPT3,* and *StFRO3* was upregulated. This suggests the negative regulation of *StbHLH47* in modulating iron. The iron content was also quantified using inductively coupled plasma mass spectrometry (ICP-MS) and found to be increased in the generated transgenic lines when compared to WT plants. Overall, this study reveals that *StbHLH47* negatively regulates the expression of iron homeostasis-related genes. *StbHLH47* edited lines exhibited decreased FCR activity, changes in phenotype, and increased iron content in the potato plants.

Key message: This study provides novel insight into the role of *StbHLH47* in modulating iron content in *Solanum tuberosum* and controlling the expression of various iron homeostasis-related genes.

1. Introduction

Iron is an essential micronutrient required for the growth and maintenance of plants, and the optimal level of iron is important to plants [11]. Iron is involved in various biochemical processes, including photosynthesis, DNA synthesis, chlorophyll synthesis, respiration, etc. Many biochemical pathways require iron as it is the prosthetic group constituent of many enzymes and proteins, such as cytochromes, and this signifies the importance of iron in the plant system [20,30]. Potato plants utilize strategy I for iron uptake, which consists of rhizosphere acidification by releasing H^+ ions. The available ferric ions are reduced to ferrous ions and finally transported inside the plant using specific transporters [11,30]. Various genes are involved in iron uptake, homeostasis, and storage. *Ferric reduction oxidase 2* (*FRO2*) reduces ferric ions to ferrous ions, as complex iron chelates are not uptaken by plants [36]. The reduced ferrous ions are uptaken by the *iron-regulated transporter 1* (*IRT1*), which belongs to the ZIP family of proteins [13]. Further, the absorbed ferrous ions are chelated by nicotianamine (NA), which transports the complex through the phloem ([19]; Bonneau et al., 2016). The ferrous-citrate complex is transported through xylem via a

☆ This article is part of a special issue entitled: "Plant Transcription Factors and their application for improving crop production" published at the journal Plant Stress.

* Corresponding author.
E-mail addresses: kashmirbio@pu.ac.in, kashmir123@gmail.com (K. Singh).

https://doi.org/10.1016/j.cpb.2024.100354
Received 1 April 2024; Received in revised form 14 May 2024; Accepted 14 May 2024
Available online 15 May 2024

ferric reductase domain 3 (FRD3)-like gene [17]. Another membrane protein family, i.e., natural resistance-associated macrophage protein (NRAMP), is involved in transporting iron in plants [12,9] (Fig. 1). However, excess free iron is associated with oxidative stress and reactive oxygen species. In plants, free iron is stored in vacuoles. The ferritin proteins were previously described as having a role in iron homeostasis and controlling iron-induced oxidative stress in plants [34,37,5].

A complex mechanism controls iron homeostasis in plants, and a number of transcription factors are involved [24,39]. Transcription factors belonging to the basic helix-loop-helix (bHLH) family have been reported to regulate iron accumulation and transport-related genes in *Arabidopsis* and rice [33,42]. This transcription factor family comprises both positive and negative regulators. *StbHLH47* is a homologue to *Arabidopsis POPEYE* (*PYE*), which belongs to the basic helix-loop-helix (bHLH) transcription factor family. The bHLH transcription factor family controls the expression of genes through their two functional domains, i.e., the DNA-binding domain and the protein-interacting domain [18]. *AtPYE* is known to regulate iron homeostasis genes under iron deprivation conditions [29]. A homolog of *AtPYE* and *StbHLH47* in rice, *OsIRO3*, is induced 20–70 fold upon Fe deficiency [25, 46]. Over-expressed *OsIRO3* lines have hypersensitivity to low Fe, and the genes induced by Fe deficiency are inhibited in these plants, suggesting that *OsIRO3* is a negative regulator of the Fe deficiency response [23,45]. *IRO3* acts as a dampener to Fe deficiency-responsive effectors like *OsNAS1/2/3*, *OsIRT1*, and *OsYSL2/15* by negatively regulating them under iron starvation [45,46,8]. *AtPYE,* which is a homolog of *StbHLH47,* is shown to repress bHLH Ib genes, i.e., *bHLH38*, *bHLH39*, *bHLH100*, and *bHLH101,* by binding to their promoters [33]. These studies signify the importance of *AtPYE* and its homologs in the iron deficiency response signaling pathway.

Micronutrient deficiencies affect more than 2 billion individuals globally [16]. Iron (Fe) deficiency affects more than 1.2 billion people globally [6]. Fe deficiency is more prevalent in developing countries where plant-based food is the major source of Fe [31]. Fe deficiency affects human health by causing anemia and resulting in impaired physical and mental health [32,7]. Potato is the third-most important crop globally and is an agriculturally relevant crop. It is easily accessible to the masses. Various studies have been done to increase the iron content of potatoes. Overexpressed lines of *ferritin* (*FER3*) and *IRT1* showed that potato plants are grown without exhibiting any Fe deficiency symptoms in calcareous soils [4]. One study showed the expression of MT (metal transporter), plasma membrane H+-ATPase, oligopeptide transporter, and germin genes increased in the potato plants (under Fe-deficient soil) and complemented the iron uptake (Xiao et al., 2015). This study contributes to understanding the role of *StbHLH47* with respect to iron homeostasis genes, which have not been investigated in the potato. Previously, we generated CRISPR/Cas9-edited potato lines using pHSE401 with up to 7 bp deletions in the target region [1]. In this report, CRISPR/Cas9-edited potato lines were analyzed for FCR activity in the edited lines. Further, the mutated lines were estimated for chlorophyll, and phenotypic changes were observed. The mutated lines were subjected to iron stress, and the expression of iron homeostasis-associated genes was measured using real-time quantitative reverse transcription PCR (qRT-PCR). The iron content was also quantified in the mutated lines using ICP-MS. Overall, our study revealed the role of *StbHLH47* potato edited lines in regulating the iron content in the potato and its negative regulation of iron homeostasis-associated genes in iron stress conditions.

2. Materials and methods

2.1. Sequence retrieval, phylogeny, and motif analysis of Iron homeostasis-related genes in the Solanaceae family

The well-characterized iron homeostasis-related protein in *Arabidopsis thaliana* was selected to characterize the iron homeostasis-related protein in the *Solanaceae* family. The protein sequences of *A. thaliana* AtPYE, AtFRO3, AtNAS4, AtZIF1, AtOPT3, AtFRD3, AtNRAM3, and AtFRO2 with accession numbers AT3G47640, AT1G23020, AT1G56430, AT5G13740, AT1G09930, AT3G08040, AT2G23150, and AT1G01580 were retrieved from the TAIR database (https://www.arabidopsis.org) [3]. The reference sequences of *A. thaliana* were Blastp searched against the *Solanum tuberosum, Solanum lycopersicum, Solanum melongena, Petunia axillaris, Capsicum annum, Nicotiana benthamina, Nicotiana tabacum, Coffea canephora,* and *Nicotiana attenuata* proteomes. The top hits were retrieved and shown in Supplementary Table S1 [10]. The retrieved sequences were aligned using ClustalW in Molecular Evolutionary Genetics Analysis MEGA 7.0 [21] (https://www.megasoftware.net/). The neighbor-joining (NJ) method with 1000 bootstrap replicates and complete deletion was used to construct the phylogenetic tree. The constructed phylogenetic tree was analyzed using the ITOL tool (https://itol.embl.de/upload.cgi) [22]. The conserved motifs of the clusters were identified using the MEME online server (https://meme.n-bcr.net/meme) [2]. The maximum number of motifs was 10, and the width of the motifs was between 50 and 100. The motifs of each cluster are shown in Supplementary Table S2.

2.2. Plant materials & regeneration

The *StbHLH47* CRISPR/Cas9-transgenic lines of *S. tuberosum* cv.

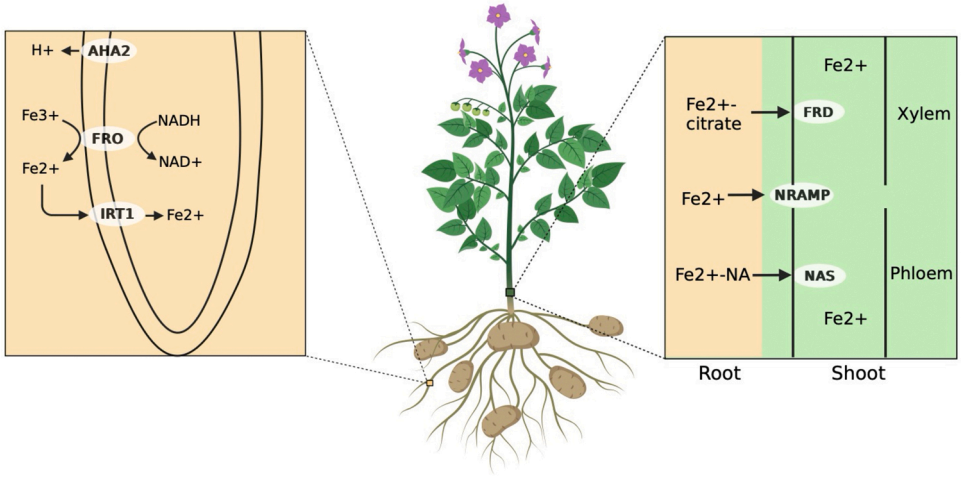

Fig. 1. Schematic representation of strategy I Iron homeostasis in plants.
(Image inspired from [11]).

Kufri jyoti were generated previously in our lab for optimizing the rapid and efficient genome editing protocol in the potato using *Rhizobium rhizogenes* (strain A4) [1]. The four transgenic lines were generated by transforming pHSE401+ gRNA in explants. The positive transformants (callus) grown on selection media were screened for mutations and analyzed. The hairy root lines were maintained and sub-cultured regularly with a photoperiod of 16 hours of light and 8 hours of darkness at a temperature of 24^0 C. For regeneration, the hairy root lines were sub-cultured on [Murashige and Skoog medium MS pH 5.8, supplemented with 3 mg/L BAP, 2 mg/L Kinetin, and 0.5 mg/L NAA]. The regenerated plantlets were sub-cultured and maintained for iron stress. For iron suficit (Fe^+) media, MS media (pH 5.8) was supplemented with 1% sucrose, 1% agar, 0.1 mM Fe-EDTA, and 0.05% MES buffer. For iron deficit (Fe^-) media, MS media (pH 5.8) was supplemented with 1% sucrose, 1% agar, 0.3 μM Ferrozine, and 0.05% MES buffer.

2.3. Iron treatment and microscopy

The regenerated plantlets were cultured on Fe^+ media [MS + 1% sucrose, 1% agar, 0.1 mM Fe-EDTA, 0.05% MES buffer] and Fe^- media [MS + 1% sucrose, 1% agar, 0.3 μM Ferrozine, 0.05% MES buffer] (Supplementary Fig. S1). The samples were obtained after 14 days from potato leaves, roots, and stems, which were preserved by snap freezing in liquid nitrogen and stored at a temperature of −80 °C for expression analysis.

To visualize the difference in the stem sections of plants, a stereo zoom microscope, the Leica S9i (Leica Microsystems, Germany), was used. The two-week-old plants (wild type (WT) and pHSE401 + gRNA L2) and (WT and pHSE401 + gRNA L5) grown on Fe^- media were imaged. Measurements were done using the analysis tool in Leica Application Suite version LAS V4.13.0.

2.4. Chlorophyll content and Ferric chelate reductase assay

The chlorophyll content of *StbHLH47*-edited and control plants was measured. The two-week-old plants were sub-cultured on Fe^+ and Fe^- media for one week. The fresh leaves were excised, snap frozen in liquid nitrogen, and crushed into fine powder. The powder was resuspended in 80% acetone and centrifuged at 10,000 g at 4^0 C for 5 minutes. The chlorophyll concentrations were determined by analyzing the absorbance values obtained via spectroscopy at wavelengths of 663.2 nm, 646.8 nm, and 470 nm [27].

The root-associated FCR activity of the *StbHLH47* edited lines was measured using spectrophotometry at 562 nm. The assay solution consisted of 0.1 mM Fe^{3+}EDTA and 0.3 mM ferrozine dissolved in distilled water. The root systems of the *StbHLH47* mutant lines and control plants were submerged in the 5 ml assay solution in the dark for 20 min [43]. The ferrous Fe(II)-ferrozine concentration was calculated using an extinction coefficient of 28.6 $mM^{-1}cm^{-1}$ [38].

2.5. RNA isolation, cDNA preparation and qRT-PCR analysis

For qRT-PCR analysis, RNA from the leaf, root, and stem was extracted after 14 days from the plants grown on Fe^+ and Fe^- media [15]. cDNA synthesis was done using the Superscript III first-strand cDNA synthesis kit (Invitrogen USA). For expression normalization, elongation factor 1 alpha (ef1α) was used as the reference gene. The expression levels of *StbHLH47* and other iron-regulating genes in mutated lines and control plants subjected to the Fe^+ and Fe^- conditions were measured using qRT-PCR. Primers used for the study were designed (Supplementary Table S3) by Primer 3 software (http://primer3.ut.ee) [40]. A Bio-Rad (CFX96) real-time PCR detection system was used to perform qRT-PCR. All the samples were taken in triplicate, and three technical replicates of each biological replicate were taken. Conditions for qRT-PCR were 95 °C for 3 min, followed by 38 cycles of 95 °C for 30 s, Tm for 30 s, and 72 °C for 30 s. The correlative expression data were calculated using the $2(^{-\Delta\Delta CT})$ method [28].

2.6. ICP-MS analysis

The potato plants (WT, pHSE401 + gRNA L2, and pHSE401 + gRNA L5) were grown in soil for 14 days, and shoots and leaf samples were collected. The samples were oven-dried (100 mg), finely powdered, and dissolved in 8 ml of HNO_3 (70%, CEM Corporation) and digested using the microwave digestion method (CEM Corporation). After dissolution, the samples were then shifted to 50-ml falcon tubes, which were filled with sterile distilled water. Before analysis, a 1:10 dilution of 2% HNO_3 in sterile distilled water was made. The dilution was filtered through a 0.22 μm nylon syringe filter to remove any contamination. Iron (Fe) concentrations in plant samples were determined using inductively coupled plasma mass spectrometry (ICP-MS, Agilent 7800). A calibration curve was prepared using a multi-element standard solution.

2.7. Statistical analysis

The data was analyzed using GraphPad Prism 9.0 (https://www.graphpad.com). The significant statistical difference was calculated between the two groups using a two-way ANOVA. The data was plotted using GraphPad Prism 9.0.

3. Results

3.1. Iron regulating genes in Solanaceae family

Iron regulation is very complex and crucial for the survival of plants and is regulated by a cluster of genes and transcription factors. To evaluate the iron-regulating genes in the *Solanaceae* family, various reference genes characterized in *A. thaliana* were used. We retrieved 70 genes across the proteomes of *S. tuberosum*, *S. lycopersicum*, *S. melongena*, *P. axillaris*, *C. annum*, *N. benthamina*, *N. tabacum*, *C. canephora*, and *N. attenuate*. We found 8 clusters having homology with the *bHLH47, OPT3, NAS4, ZIF1, FRO3, FRO2, FRD3,* and *NRAM3* are involved in iron homeostasis in the *Solanaceae* family (Fig. 2a).

To further confirm that the retrieved sequences have similar functions, domain analysis and motif analysis were done. We found that all the clusters contain their own signature domains specific to their functionality. The bHLH47 sequences consist of the signature HLH domain (IPR011598). Similarly, NAS4, FRO2, OPT3, FRO3, FRD3, ZIF1, and NRAM3 sequences in the cluster consist of their signature domains, i.e., the NAS domain (IPR004298), ferric reductase domain (IPR013130)/ FAD-binding domain (IPR017927), oligopeptide transporter domain (IPR004813), ferric reductase domain (IPR013130), MATE family domain (IPR002528), MFS domain (IPR020846), and NRAMP family domain (IPR001046), respectively. The clusters were analyzed for their motifs, and the bHLH47 cluster contains similar motifs across all the sequences (Fig. 2b). While in clusters like NRAM3, NAS4, OPT3, ZIF1, and FRO2, all the sequences contain major motifs, suggesting their importance in the functioning of these genes, a few motifs are specific to certain sequences (Fig. 2b).

3.2. Genotype analysis of the generated mutants

A total of 32 probable sites were identified previously in *StbHLH47* by [1], starting from the 5' UTR region. The target sequence was selected on the first exon, which was adjacent upstream to the start codon of the gene. The crRNA duplex was inserted into the pHSE401 vector and was under the control of the AtU6 promoter. A total of 26 transformed lines were screened for mutations. Out of 26, four lines (pHSE401 + gRNA L2, pHSE401 + gRNA L5, pHSE401 + gRNA L6, and pHSE401 + gRNA L7) showed deletion of 2–7 nucleotide bp when compared to the WT [1]. The transgenic lines pHSE401 + gRNA L2 showed the maximum deletion, i.e., 7 nucleotide bp. The transgenic

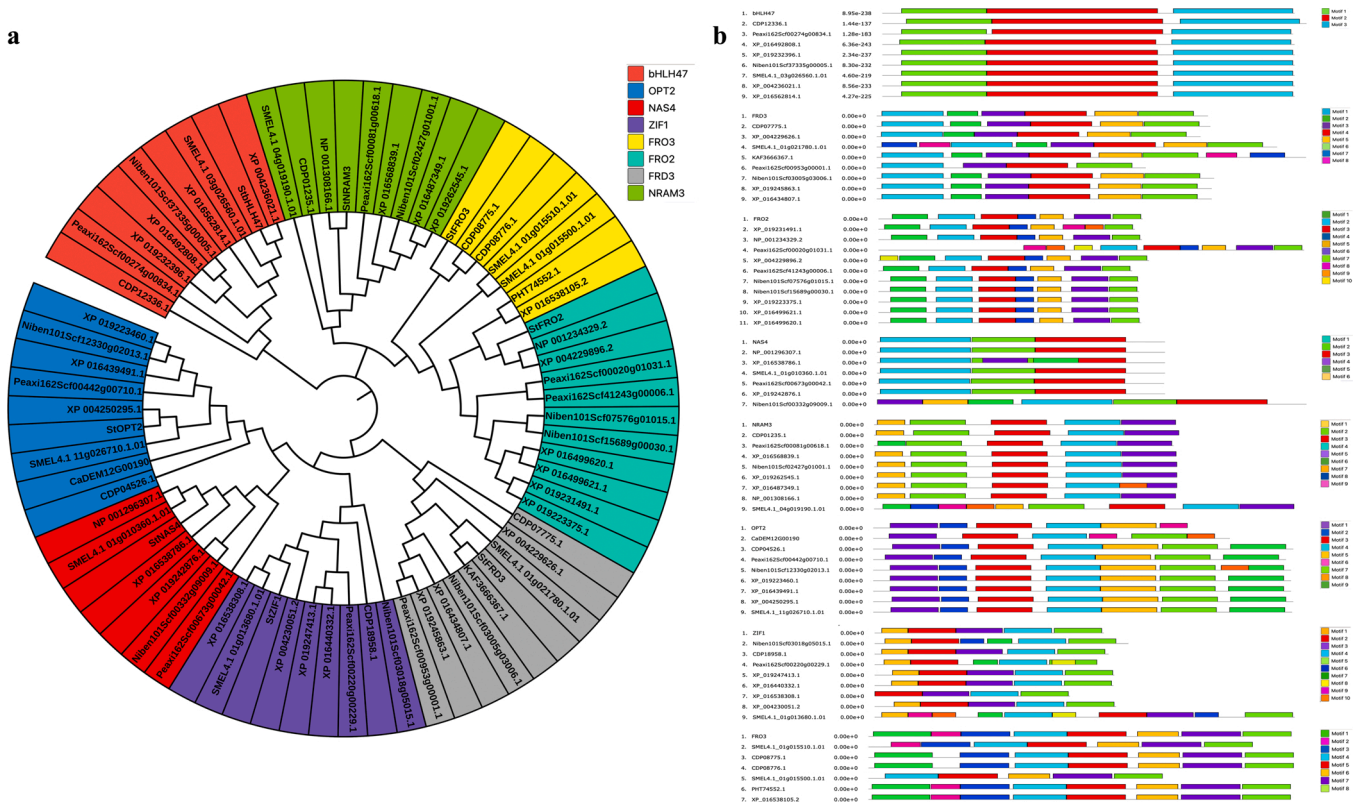

Fig. 2. : Phylogenetic tree and motif composition of iron homeostasis genes in *Solanaceae* family. **a)** Phylogenetic tree of iron homeostasis related genes in *Solanaceae* family. **b)** Conserved motifs of bHLH47, FRD3, FRO2, NAS4, NRAM3, OPT3, ZIF1, and FRO3 represented in different colored boxes across the members of *Solanaceae* family.

lines pHSE401 + gRNA L5 and pHSE401 + gRNA L6 showed deletions of 2 nucleotide bp in the same region [1]. Since the target region was adjacent to exon 1 and lies in the 5' UTR region as well, it was checked for probable change in the open reading frame. It was found that none of the four lines (pHSE401 + gRNA L2, pHSE401 + gRNA L5, pHSE401 + gRNA L6, and pHSE401 + gRNA L7) had any changes in frame.

Fig. 3. : Regeneration stages of *StbHLH47* line 2 and line 5 hairy roots **a & e)** onto MS medium, **b & f)** onto regeneration medium containing MS+ 3 mg/L BAP, 2 mg/L Kin, 0.5 mg/L NAA, **c & g)** onto MS medium, **d & h)** in pots. Morphological differences in trichomes **i)** WT plant under Fe^{-} condition, **j)** pHSE401+ gRNA L2 plant under Fe^{-} condition, **k)** WT plant under Fe^{-} condition, **l)** pHSE401+ gRNA L5 plant under Fe^{-} condition. Red line in Fig. 3(i-l) is the 1 mm scale.

However, these mutations can repress the expression of *StbHLH47*, and the analyzed hairy root lines were regenerated and further investigated for their phenotype and other properties.

3.3. Transgenic StbHLH47 lines exhibit altered phenotype

The regeneration was optimized for the CRISPR/Cas9-edited transgenic hairy root lines of *StbHLH47*. Out of the four transgenic lines, pHSE401 + gRNA L2 and pHSE401 + gRNA L5 were successfully regenerated into plants (Fig. 3a–h). In the knockdown lines of *StbHLH47,* we observed deformations in the trichomes both in Fe^{+} and Fe^{-} medium. The trichomes of WT plants grown on Fe^{-} medium were long and scattered across the stem. However, in the *StbHLH47* edited lines grown on Fe^{-} medium, the trichomes were short and thin when compared to the WT plants, which was not reported earlier (Fig. 3i–l). The trichomes of WT and *StbHLH47* lines grown on Fe^{+} medium are shown in supplementary Fig. S2.

We also found that the chlorophyll a, chlorophyll *b*, and total chlorophyll content were lowered in *StbHLH47* lines when compared with the WT plants in both Fe^{+} and Fe^{-} conditions. However, the chlorophyll content decreased in the Fe^{-} conditions, both in WT and mutant plants (Fig. 4a–c). The carotenoid content was also estimated, and the *StbHLH47* mutants have lower carotenoid content when compared with the WT plants in Fe^{+} and Fe^{-} conditions (Fig. 4d).

The *StbHLH47* expression levels were analyzed and found to be elevated in the WT plants when subjected to the Fe^{-} conditions (Fig. 5a). The expression of various genes involved in iron homeostasis, i.e., *StNRAM3*, *StOPT3*, *StFRD3*, *StFRO2*, *StNAS4*, *StFRO3*, and *StZIF1,* was checked in WT plants under Fe^{-}conditions. We found elevated expression levels in WT plants grown in Fe^{-} medium, with the highest fold change in *StFRO2*, *StZIF1*, and *StFRO3* (Fig. 5a). This shows that the expression of these genes is elevated under the Fe^{-} conditions.

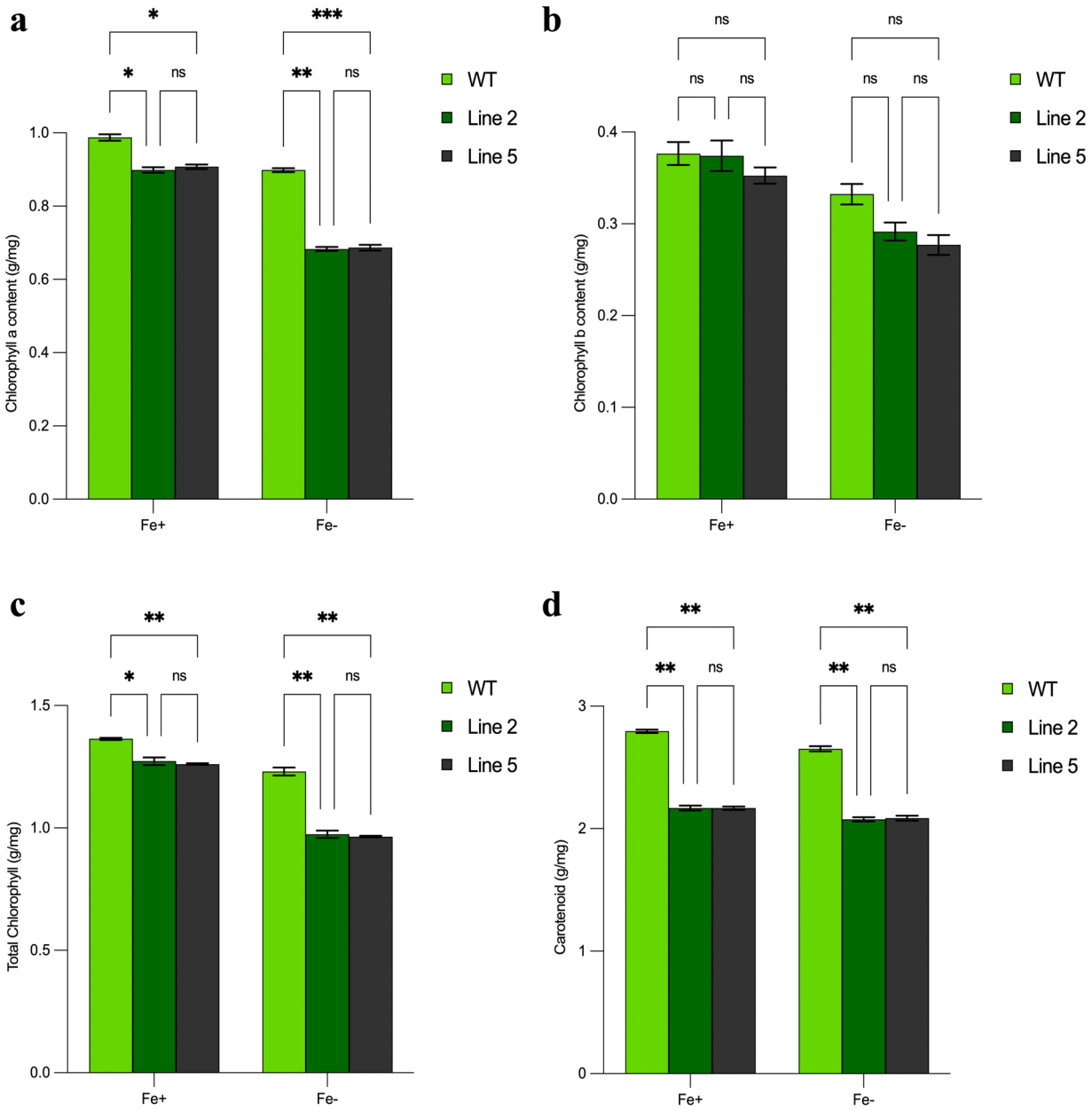

Fig. 4. : Estimation of pHSE401+ gRNA L2 and pHSE401+ gRNA L5 lines for **a)** Chlorophyll a, **b)** Chlorophyll b, **c)** Total chlorophyll, and **d)** Carotenoid. Error bars denote the SD of the mean (n=3). Asterisks denote significance by comparing pHSE401+ gRNA L2, and pHSE401+ gRNA L5 lines with the WT using a two-way ANOVA ($p<0.0001$).

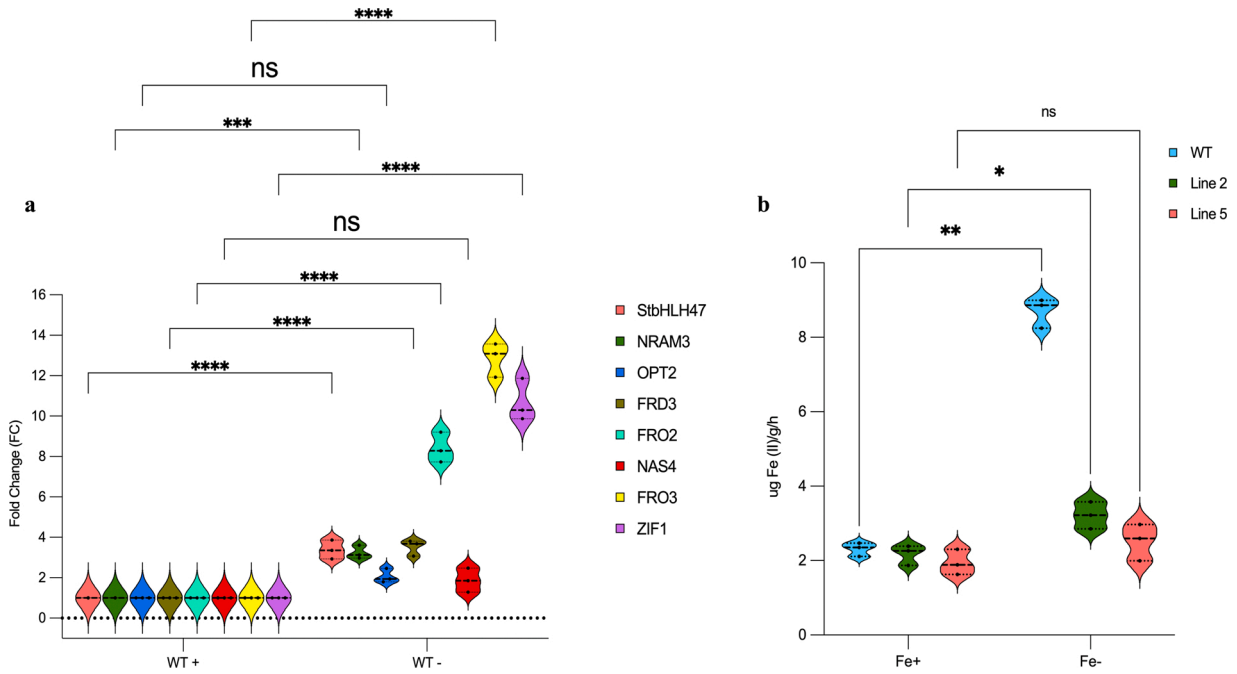

Fig. 5. : Real-time quantitative reverse transcription-polymerase chain reaction (qRT-PCR) analyses of **a)** *StbHLH47, NRAM3, OPT3, FRD3, FRO2, NAS4, FRO3,* and *ZIF1* in WT plants under Fe^{-} conditions. Violin plots denote the SD of the mean (n=3). Asterisks denote significance by comparing the FC of iron homeostasis genes in WT plants under Fe^{+} and Fe^{-} conditions using a two-way ANOVA ($p<0.0001$). **b)** Ferric chelate reductase (FCR) activity of pHSE401+ gRNA L2 and pHSE401+ gRNA L5 wrt WT. Violin plots denote the SD of the mean (n=3). Asterisks denote significance by comparing the FCR activity of pHSE401+ gRNA L2, pHSE401+ gRNA L5, and WT in Fe^{+} and Fe^{-} medium using a two-way ANOVA ($p<0.001$).

3.4. Role of StbHLH47 in controlling iron reductase activity

To study the role of *StbHLH47* on the FCR activity of the potato roots, a ferrozine assay was performed under Fe^{+} and Fe^{-} conditions. We observed increased iron reductase activity in both WT and transgenic lines, but the transgenic lines exhibited decreased iron reductase activity when compared to the WT (Fig. 5b). This suggests that *StbHLH47* edited lines affect *StFRO2*, which results in lowered FCR in the potato roots. These results implied further validation of the expression levels of *StFRO2* in knockdown *StbHLH47* potato lines by qRT-PCR (Fig. 6a).

3.5. Expression profiling of iron homeostasis-related genes in StbHLH47 mutants

To further confirm the effects of *StbHLH47* on the expression levels of iron homeostasis-related genes, qRT-PCR was performed. The expression levels of eight genes, i.e., *StbHLH47*, *StFRO3*, *StNAS4*, *StZIF1*, *StOPT3*, *StFRD3*, *StNRAM2*, and *StFRO2*, were analyzed in the leaf, root, and stem tissues of the edited lines. The expression levels of *StFRO3* and *StZIF1* were elevated throughout in the *StbHLH47* mutants. However, the fold change (FC) was further increased in leaf, root, and stem when

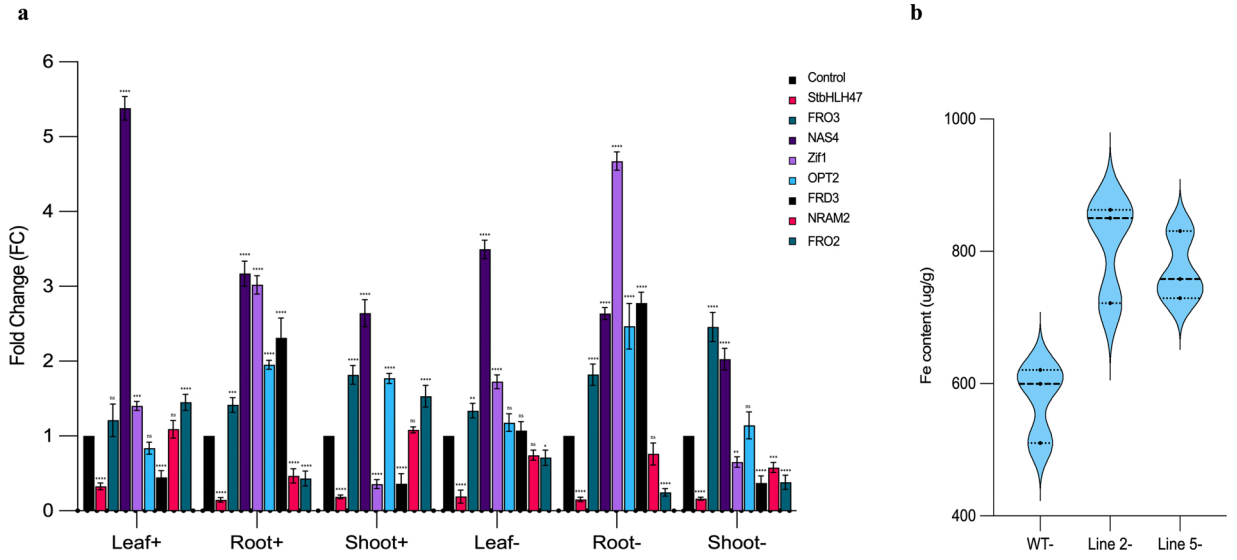

Fig. 6. : a) Real-time quantitative reverse transcription-polymerase chain reaction (qRT-PCR) analyses of *StbHLH47, FRO3, NAS4, ZIF1, OPT3, FRD3, NRAM2,* and *FRO2* in transgenic plants in leaf, root, and stem tissues under Fe^{+} and Fe^{-} conditions. Error bars denote the SD of the mean (n=3). Asterisks denote significance by comparing the FC of iron homeostasis genes in Fe^{+} and Fe^{-} medium in leaf, root, and shoot with internal control (EF1 α) using a two-way ANOVA ($p<0.0001$). **b)** Inductively coupled plasma- Mass spectroscopy (ICP-MS) analysis of pHSE401+ gRNA L2 and pHSE401+ gRNA L5. Violin plots denote the SD of the mean (n=3).

the plants were subjected to the Fe$^-$ conditions. *StNAS4* was also elevated with FC 5.38, 3.17, and 2.64 in leaf, root, and stem, respectively, under Fe$^+$ conditions. But when subjected to the Fe$^-$ conditions, FC changes to 3.49, 2.63, and 2.02 in leaf, root, and stem, respectively (Fig. 6a).

The expression of *StFRO2* was also evaluated, and it was found that the expression decreased in root with FC 0.43 under the Fe$^+$ condition and in the Fe$^-$ condition FC was 0.24 (Fig. 6a). This shows that edited *StbHLH47* transgenic lines affected the expression of *StFRO2,* and due to the reduced expression in roots, the ferric chelate reductase activity was also reduced in the *StbHLH47* knockdown lines.

The *StOPT3* was elevated in roots with FC 1.95 and FC 2.46 in both Fe$^+$ and Fe$^-$ conditions, respectively. Similarly, the expression of *StFRD3* was also elevated in roots with FC 2.31 under the Fe$^+$ condition and increased to FC 2.77 in roots under the Fe$^-$ condition (Fig. 6a). These results signify the importance of *StbHLH47* in regulating iron homeostasis-related genes.

3.6. Iron content of StbHLH47 mutants

To determine the effect of *StbHLH47* on the iron content, we quantified the iron content of both the mutated lines, i.e., pHSE401 + gRNA L2 and pHSE401 + gRNA L5. Iron quantification of potato shoots using ICP-MS showed that pHSE401 + gRNA L2 and pHSE401 + gRNA L5 exhibit an increased amount of iron when compared to the WT plants. We found that pHSE401 + gRNA L2 had an iron concentration of 811 μg/g and pHSE401 + gRNA L5 had an iron concentration of 772 μg/g, while the WT plant had a concentration of 576 μg/g of iron content (Fig. 6b). These results suggest that *StbHLH47* is responsible for maintaining iron levels in plants and controls them negatively.

4. Discussion

Iron is an important micronutrient, and its deficiency is harmful to plant growth and development. Plants respond to iron stress in both iron deficiency and iron sufficiency conditions [11]. Plants can detect iron deficiency conditions and respond by modulating iron homeostasis-related genes. Various transcription factors play regulatory roles in iron deficiency signaling pathways. The basic/helix-loop-helix (bHLH) is the second largest transcription factor superfamily and is known to modulate the expression of iron homeostasis-related genes [14,25,35]. The *StbHLH47* belongs to the bHLH transcription factor superfamily and is a homolog to the *AtPYE* and *OsIRO3* in potatoes. Knocked-down *AtPYE* mutants were reported to increase the sensitivity to the iron deficiency response and negatively control iron homeostasis-related genes [29]. The role of *StbHLH47* in association with modulating iron has not been explored in potatoes.

In this study, CRISPR/Cas9 knocked-down lines were successfully regenerated into plants from the hairy root callus. Using the developed lines, we showed that *StbHLH47* is important for the iron deficiency response in the potatoes and modulates iron content in the potato plant. The potato uses strategy I for the uptake of iron and utilizes a series of genes for it. Under iron deficiency conditions, plant growth, development, and young leaves are affected. The StbHLH47 lines exhibited reduced chlorophyll and carotenoid content, which was also affected in *Arabidopsis* when *AtPYE* (homolog to the *StbHLH47*) was silenced [29]. The expression of *StbHLH47* was checked and found elevated in the WT plants under the Fe$^-$ conditions. The *StbHLH47* lines were analyzed for iron reductase activity, which is one of the typical indicators of iron deficiency response [43]. The iron reductase activity, which is controlled by *FRO2,* is elevated under the Fe$^-$ conditions. *FRO2* reduces ferric ions to ferrous ions, which are taken up by the membrane transporters [36]. The iron reductase activity was found to be reduced in the *StbHLH47* lines, suggesting the role of *StbHLH47* in controlling *StFRO2,* which was further confirmed by the reduced expression levels of *StFRO2*. The bHLH TFs are known to control various plant developmental processes, and we have observed decreased trichome length in the *StbHLH47* lines (Fig. 3i-l). Previous studies have also reported defects in root development, decreased root length, and shoot biomass in *OsIRO3* and *AtPYE* [33,42].

Previous studies have reported that *AtPYE* regulates the expression of *AtNAS4, AtFRO3,* and *AtZIF1* by directly binding to their promoters [29]. *AtPYE* was further explored to reveal that it negatively controls the expression of bHLH Ib genes, i.e., *bHLH38, bHLH39, bHLH100,* and *bHLH101,* by binding directly to their promoters. The transcriptional activation of *bHLH* IVc genes, i.e., *bHLH104, bHLH105,* and *bHLH115,* was repressed indirectly by *AtPYE* [33]. Moreover, bHLH subgroup Ib members (*bHLH38*, *bHLH39*, *bHLH100*, and *bHLH101)* positively regulate the expression of *IRT1* and *FRO2* by forming heterodimers with *FIT* under iron deficiency [41,44]. *bHLH34, bHLH104, bHLH105,* and *bHLH115* positively regulate *bHLH38, bHLH39, bHLH100, bHLH101,* and *PYE* (the homolog of *StbHLH47*) [24,26,45].

In our study, expression levels of *StFRO3*, *StNAS4*, and *StZIF1* were elevated in the knockdown lines, while the expression levels of *StNRAM3*, and *StFRO2* were decreased. *AtPYE* can bind to the promoter regions of *FRO3*, *NAS4*, and *ZIF1* [29]. This suggests that *StbHLH47* can control the expression of *StFRO3*, *StNAS4*, and *StZIF1* in the potatoes, which is in compliance with the previous studies. The iron content was estimated using ICP-MS and found that the *StbHLH47* lines contain increased iron levels in the shoot when compared to the WT plants. *OsIRO3* knockout lines also showed increased iron content in rice, while overexpressing lines showed decreased iron content [42,46]. However, *FRO3, NAS4, ZIF1, FRO2, NRAM3, OPT3,* and *FRD3* are important genes in iron homeostasis and well-characterized in other plants but not in the potatoes, so they should be explored in the potatoes.

Our study suggests the importance of *StbHLH47* in regulating the expression of iron homeostasis-related genes in potatoes. Hence, more studies should be done to decipher the regulatory relationship of Fe deficiency with bHLH transcription factors in potatoes. Overall, *StbHLH47* negatively controls the iron levels in the potatoes, which was confirmed using CRISPR/cas9 knockout lines. The expression of *StFRO2* was reduced in transgenic lines, which led to decreased iron reductase activity. The negative regulation of iron content by *StbHLH47* indicates its importance in modulating iron in potatoes.

5. Conclusion

In conclusion, our results identified the negative regulation of iron by *StbHLH47* under iron stress conditions in the potato, which was not studied earlier. The CRISPR/Cas9-generated knocked-down lines of *StbHLH47* exhibited changes in the trichome number and length. The chlorophyll and carotenoid content of the knocked-down lines decreased when compared to the WT plants. Ferric reductase chelate activity was checked in the transgenic lines, which was also reduced by targeting *StbHLH47*. The expression of iron homeostasis-related genes was analyzed in *S. tuberosum,* and *StFRO3*, *StZIF1*, *StbHLH47*, and *StFRO2* were upregulated in WT plants under the Fe$^-$ conditions. These results demonstrated the importance of these genes in iron homeostasis, which was also checked in the *StbHLH47* lines under Fe$^-$ conditions in different tissues. The iron content was also checked, and the *StbHLH47* lines showed increased iron content when compared to the WT plants. These results gave insight into the role of *StbHLH47* in regulating iron content and provided a knowledge-domain for further exploring the iron homeostasis pathway in potatoes. The relationship between *StbHLH47* and *StZIF1*, *StFRO3, StNAS4,* and *StOPT3* can further be explored using complementation studies to determine their roles.

Author contribution

KS; conceived the idea, designed the experiments, analyzed the results, and finalized the manuscript. HC performed assays, qRT-PCR, analyzed the data, and wrote the manuscript. HC and AA generated CRISPR/Cas9 edited lines, plant tissue culture. A; sub-culturing,

compiled the data; AP; performed ICP-MS and analyzed the results. SKU: analyzed the data and wrote the manuscript.

Funding

The authors are thankful to the Department of Biotechnology (DBT), Government of India for providing the resources and financial support for the study.

Declaration of Competing Interest

The authors declare that they have no conflict of interest.

Data availability

No data was used for the research described in the article.

Acknowledgements

The authors are thankful to the Department of Biotechnology, Panjab University, Chandigarh, for providing research facilities. The authors are thankful to the Department of Biotechnology of the Government of India for the research grant. HC is thankful to the Council of Scientific and Industrial Research (CSIR) for awarding junior and senior research fellowships. A is grateful to the University Grants Commission (UGC), New Delhi, for providing the junior and senior research fellowships.

Appendix A. Supporting information

Supplementary data associated with this article can be found in the online version at doi:10.1016/j.cpb.2024.100354.

References

[1] A. Alok, H. Chauhan, N. Kaushal, Aiana, K. Singh, Rapid and efficient CRISPR/Cas9-mediated genome editing in potato via hairy root induction, Vitr. Cell. Dev. Biol. -Plant *59* (1) (2023) 83–94, https://doi.org/10.1007/s11627-022-10318-0.

[2] T.L. Bailey, J. Johnson, C.E. Grant, W.S. Noble, The MEME suite, Nucleic Acids Res. 43 (2015) 39–49, https://doi.org/10.1093/nar/gkv416.

[3] Tanya Z. Berardini, Leonore Reiser, Donghui Li, Yarik Mezheritsky, Robert Muller, Emily Strait, Eva Huala, The Arabidopsis Information Resource: Making and mining the "gold standard" annotated reference plant genome, genesis *53* (8) (2015) 474–485, https://doi.org/10.1002/dvg.22877.

[4] G.A. Boamponsem, D.W.M. Leung, C. Lister, Insights into resistance to Fe deficiency stress from a comparative study of in vitro-selected novel Fe-efficient and Fe-inefficient potato plants, Front. Plant Sci. 8 (2017) 1581, https://doi.org/10.3389/fpls.2017.01581.

[5] J.F. Briat, C. Duc, K. Ravet, F. Gaymard, Ferritins and iron storage in plants, Biochim. Et. Biophys. Acta (BBA)-Gen. Subj. *1800* (8) (2010) 806–814, https://doi.org/10.1016/j.bbagen.2009.12.003.

[6] C. Camaschella, Iron deficiency, Blood 133 (2019) 30–39, https://doi.org/10.1182/blood-2018-05-815944.

[7] M.D. Cappellini, K.M. Musallam, A.T. Taher, Iron deficiency anaemia revisited, J. Intern. Med. 287 (2020) 153–170, https://doi.org/10.1111/joim.13004.

[8] O. Carey-Fung, M. O'Brien, J.T. Beasley, A.A. Johnson, A model to incorporate the bHLH transcription factor OsIRO3 within the rice iron homeostasis regulatory network, Int. J. Mol. Sci. *23* (3) (2022) 1635, https://doi.org/10.3390/ijms23031635.

[9] L. Castaings, A. Caquot, S. Loubet, C. Curie, The high-affinity metal transporters NRAMP1 and IRT1 team up to take up iron under sufficient metal provision, Sci. Rep. *6* (1) (2016) 37222, https://doi.org/10.1038/srep37222.

[10] H. Chauhan, K. Singh, Genome-wide identification of 2-oxoglutarate and Fe (II)-dependent dioxygenase family genes and their expression profiling under drought and salt stress in potato, PeerJ *11* (2023) e16449, https://doi.org/10.7717/peerj.16449.

[11] J.M. Connorton, J. Balk, J. Rodríguez-Celma, Iron homeostasis in plants–a brief overview, Metallomics *9* (7) (2017) 813–823, https://doi.org/10.1039/c7mt00136c.

[12] C. Curie, J.M. Alonso, M.L. JEAN, J.R. Ecker, J.F. Briat, Involvement of NRAMP1 from Arabidopsis thaliana in iron transport, Biochem. J. *347* (3) (2000) 749–755, https://doi.org/10.1042/bj3470749.

[13] Eide D., Broderius M., Fett J., Guerinot M.L. (1996) A novel iron-regulated metal transporter from plants identified by functional expression in yeast. Proceedings of the National Academy of Sciences *93*(11), pp.5624-5628. https://doi.org/103.155.138.209.

[14] F. Gao, C. Dubos, Transcriptional integration of plant responses to iron availability, J. Exp. Bot. *72* (6) (2021) 2056–2070, https://doi.org/10.1093/jxb/eraa556.

[15] S. Ghawana, A. Paul, H. Kumar, A. Kumar, H. Singh, P.K. Bhardwaj, A. Rani, R. S. Singh, J. Raizada, K. Singh, S. Kumar, An RNA isolation system for plant tissues rich in secondary metabolites, *4*, BMC Res. Notes 4 (1) (2011) 1–5, https://doi.org/10.1186/1756-0500-4-85.

[16] T. Gödecke, A.J. Stein, M. Qaim, The global burden of chronic and hidden hunger: Trends and determinants, Glob. Food Secur. 17 (2018) 21–29, https://doi.org/10.1016/j.gfs.2018.03.004.

[17] L.S. Green, E.E. Rogers, FRD3 controls iron localization in Arabidopsis, Plant Physiol. *136* (1) (2004) 2523–2531, https://doi.org/10.1104/pp.104.045633.

[18] S.I. Karchner, W.H. Powell, M.E. Hahn, Identification and Functional Characterization of Two Highly Divergent Aryl Hydrocarbon Receptors (AHR1 and AHR2) in the TeleostFundulus heteroclitus: EVIDENCE FOR A NOVEL SUBFAMILY OF LIGAND-BINDING BASIC HELIX LOOP HELIX-PER-ARNT-SIM (bHLH-PAS) FACTORS, J. Biol. Chem. *274* (47) (1999) 33814–33824, https://doi.org/10.1074/jbc.274.47.33814.

[19] M. Klatte, M. Schuler, M. Wirtz, C. Fink-Straube, R. Hell, P. Bauer, The analysis of Arabidopsis nicotianamine synthase mutants reveals functions for nicotianamine in seed iron loading and iron deficiency responses, Plant Physiol. *150* (1) (2009) 257–271, https://doi.org/10.1104/pp.109.136374.

[20] C.A. Krohling, F.J. Eutrópio, A.A. Bertolazi, L.B. Dobbss, E. Campostrini, T. Dias, A. C. Ramos, Ecophysiology of iron homeostasis in plants, Soil Sci. Plant Nutr. *62* (1) (2016) 39–47, https://doi.org/10.1080/00380768.2015.1123116.

[21] S. Kumar, G. Stecher, K. Tamura, J. Dudley, MEGA7: Molecular Evolutionary Genetics Analysis Version 7.0 for Bigger Datasets, Mol. Biol. Evol. 33 (2016) 1870–1874, https://doi.org/10.1093/molbev/msw054.

[22] I. Letunic, P. Bork, Bioinformatics applications note Phylogenetics Interactive Tree Of Life (iTOL): an online tool for phylogenetic tree display and annotation, Bioinformatics 23 (2007) 127–128, https://doi.org/10.1093/bioinformatics/btl529.

[23] C. Li, Y. Li, P. Xu, G. Liang, OsIRO3 negatively regulates Fe homeostasis by repressing the expression of OsIRO2, Plant J. *111* (4) (2022) 966–978, https://doi.org/10.1111/tpj.15864.

[24] X. Li, H. Zhang, Q. Ai, G. Liang, D. Yu, Two bHLH transcription factors, bHLH34 and bHLH104, regulate iron homeostasis in Arabidopsis thaliana, Plant Physiol. *170* (4) (2016) 2478–2493, https://doi.org/10.1104/pp.15.01827.

[25] G. Liang, Iron uptake, signaling, and sensing in plants, Plant Commun. (2022), https://doi.org/10.1016/j.xplc.2022.100349.

[26] G. Liang, H. Zhang, X. Li, Q. Ai, D. Yu, bHLH transcription factor bHLH115 regulates iron homeostasis in Arabidopsis thaliana, J. Exp. Bot. *68* (7) (2017) 1743–1755, https://doi.org/10.1093/jxb/erx043.

[27] H.K. Lichtenthaler, Chlorophylls and carotenoids: pigments of photosynthetic biomembranes, Methods Enzymol. Vol. 148 (1987) 350–382, https://doi.org/10.1016/0076-6879(87)48036-1.

[28] K.J. Livak, T.D. Schmittgen, Analysis of relative gene expression data using real-time quantitative PCR and the 2-ΔΔCT method, Methods 25 (2001) 402–408, https://doi.org/10.1006/meth.2001.1262.

[29] T.A. Long, H. Tsukagoshi, W. Busch, B. Lahner, D.E. Salt, P.N. Benfey, The bHLH transcription factor POPEYE regulates response to iron deficiency in Arabidopsis roots, Plant Cell 22 (7) (2010) 2219–2236, https://doi.org/10.1105/tpc.110.074096.

[30] L. Mahawar, K.P. Ramasamy, A. Pandey, S.M. Prasad, Iron deficiency in plants: an update on homeostasis and its regulation by nitric oxide and phytohormones, Plant Growth Regul. *100* (2) (2023) 283–299, https://doi.org/10.1007/s10725-022-00853-6.

[31] S.R. Pasricha, H. Drakesmith, J. Black, D. Hipgrave, B.A. Biggs, Control of iron deficiency anemia in low- and middle-income countries, Blood 121 (2013) 2607–2617, https://doi.org/10.1182/blood-2012-09-453522.

[32] L. Pivina, Y. Semenova, M.D. Doşa, M. Dauletyarova, G. Bjørklund, Iron Deficiency, Cognitive Functions, and Neurobehavioral Disorders in Children, J. Mol. Neurosci. 68 (2019) 1–10, https://doi.org/10.1007/s12031-019-01276-1.

[33] M.N. Pu, G. Liang, The transcription factor POPEYE negatively regulates the expression of bHLH Ib genes to maintain iron homeostasis, J. Exp. Bot. *74* (8) (2023) 2754–2767, https://doi.org/10.1093/jxb/erad057.

[34] K. Ravet, B. Touraine, J. Boucherez, J.F. Briat, F. Gaymard, F. Cellier, Ferritins control interaction between iron homeostasis and oxidative stress in Arabidopsis, Plant J. *57* (3) (2009) 400–412, https://doi.org/10.1111/j.1365-313X.2008.03698.x.

[35] N. Riaz, M.L. Guerinot, All together now: regulation of the iron deficiency response, J. Exp. Bot. *72* (6) (2021) 2045–2055, https://doi.org/10.1093/jxb/erab003.

[36] N.J. Robinson, C.M. Procter, E.L. Connolly, M.L. Guerinot, A ferric-chelate reductase for iron uptake from soils, Nature *397* (6721) (1999) 694–697.

[37] H. Roschzttardtz, G. Conéjéro, C. Curie, S. Mari, Identification of the endodermal vacuole as the iron storage compartment in the Arabidopsis embryo, Plant Physiol. *151* (3) (2009) 1329–1338, https://doi.org/10.1104/pp.109.144444.

[38] W. Schmidt, J. Tittel, A. Schikora, Role of hormones in the induction of iron deficiency responses in Arabidopsis roots, Plant Physiol. *122* (4) (2000) 1109–1118, https://doi.org/10.1104/pp.122.4.1109.

[39] H. Song, Q. Geng, X. Wu, M. Hu, M. Ye, X. Yu, Y. Chen, J. Xu, L. Jiang, S. Cao, The transcription factor MYC1 interacts with FIT to negatively regulate iron homeostasis in Arabidopsis thaliana, Plant J. *114* (1) (2023) 193–208, https://doi.org/10.1111/tpj.16130.

[40] A. Untergasser, I. Cutcutache, T. Koressaar, J. Ye, B.C. Faircloth, M. Remm, S. G. Rozen, Primer3-new capabilities and interfaces, e115-e115, Nucleic Acids Res. *40* (15) (2012), https://doi.org/10.1093/nar/gks596.

[41] H.Y. Wang, M. Klatte, M. Jakoby, H. Bäumlein, B. Weisshaar, P. Bauer, Iron deficiency-mediated stress regulation of four subgroup Ib BHLH genes in Arabidopsis thaliana, Planta *226* (2007) 897–908, https://doi.org/10.1007/s00425-007-0535-x.

[42] W. Wang, J. Ye, Y. Ma, T. Wang, H. Shou, L. Zheng, OsIRO3 plays an essential role in iron deficiency responses and regulates iron homeostasis in rice, Plants *9* (9) (2020) 1095, https://doi.org/10.3390/plants9091095.

[43] Y. Yi, M.L. Guerinot, Genetic evidence that induction of root Fe (III) chelate reductase activity is necessary for iron uptake under iron deficiency, Plant J. *10* (5) (1996) 835–844, https://doi.org/10.1046/j.1365-313X.1996.10050835.x.

[44] Y. Yuan, H. Wu, N. Wang, J. Li, W. Zhao, J. Du, D. Wang, H.Q. Ling, FIT interacts with AtbHLH38 and AtbHLH39 in regulating iron uptake gene expression for iron homeostasis in Arabidopsis, Cell Res. *18* (3) (2008) 385–397, https://doi.org/10.1038/cr.2008.26.

[45] J. Zhang, B. Liu, M. Li, D. Feng, H. Jin, P. Wang, J. Liu, F. Xiong, J. Wang, H. B. Wang, The bHLH transcription factor bHLH104 interacts with IAA-LEUCINE RESISTANT3 and modulates iron homeostasis in Arabidopsis, Plant Cell *27* (3) (2015) 787–805, https://doi.org/10.1105/tpc.114.132704.

[46] L. Zheng, Y. Ying, L. Wang, F. Wang, J. Whelan, H. Shou, Identification of a novel iron regulated basic helix-loop-helix protein involved in Fe homeostasis in Oryza sativa, BMC Plant Biol. *10* (2010) 1–9, https://doi.org/1471-2229/10/166.